# Measuring macromolecular diffusion using heteronuclear multiple-quantum pulsed-field-gradient NMR

Andrew J. Dingley[a], Joel P. Mackay[a], Graeme L. Shaw[c], Brett D. Hambly[b] and Glenn F. King[a,*]

*Departments of [a]Biochemistry and [b]Pathology, University of Sydney, Sydney, NSW 2006, Australia*
*[c]Department of Biochemistry, University of Oxford, Oxford OX1 3QU, U.K.*

## Summary

We have previously shown that ^{1}H pulsed-field-gradient (PFG) NMR spectroscopy provides a facile method for monitoring protein self-association and can be used, albeit with some caveats, to measure the apparent molecular mass of the diffusant [Dingley et al. (1995) *J. Biomol. NMR*, **6**, 321–328]. In this paper we show that, for ^{15}N-labelled proteins, selection of [1]H-^{15}N multiple-quantum (MQ) coherences in PFG diffusion experiments provides several advantages over monitoring ^{1}H single-quantum (SQ) magnetization. First, the use of a gradient-selected MQ filter provides a convenient means of suppressing resonances from both the solvent and unlabelled solutes. Second, [1]H-^{15}N zero-quantum coherence dephases more rapidly than ^{1}H SQ coherence under the influence of a PFG. This allows the diffusion coefficients of larger proteins to be measured more readily. Alternatively, the gradient length and/or the diffusion delay may be decreased, thereby reducing signal losses from relaxation. In order to extend the size of macromolecules to which these experiments can be applied, we have developed a new MQ PFG diffusion experiment in which the magnetization is stored as longitudinal two-spin order for most of the diffusion period, thus minimizing sensitivity losses due to transverse relaxation and J-coupling evolution.

## Introduction

A prerequisite for protein structure determination using NMR spectroscopy is that the protein is monodisperse and does not self-associate to form complexes larger than 35–40 kDa (King and Mackay, 1996). Hence, one of the first steps in such studies is to determine conditions that prevent aggregation at millimolar protein concentrations. Conventional techniques for monitoring the self-association of biological macromolecules, such as analytical ultracentrifugation, can be difficult to apply when dealing with the high concentrations of protein required for NMR structural studies. In some instances, sedimentation equilibrium studies are not possible because the solvent and solute densities are equivalent.

It has recently been demonstrated that ^{1}H pulsed-field-gradient (PFG) NMR spectroscopy provides a facile alternative to conventional techniques for monitoring protein self-association (Altieri et al., 1995; Dingley et al.,

1995). This technique involves measurement of the translational diffusion coefficient ($D_T$) by sandwiching a delay for molecular diffusion between a pair of PFGs. The extent of refocussing of the magnetization by the second PFG depends on the rate of molecular diffusion. Complete refocussing is achieved only if the molecule does not undergo translational diffusion in the time between the two gradient pulses, otherwise the signal is attenuated by an amount that depends on $D_T$.

The measured $D_T$, albeit with some caveats, can be used to calculate the apparent molecular mass ($M_{app}$) of the diffusing species (Dingley et al., 1995). For example, we previously showed that the 18.7 kDa calcium-binding protein myosin light chain two (MLC2) self-associates, even at submillimolar concentrations, forming aggregates of ~60 kDa. However, addition of the non-denaturing detergent 3-[(3-cholamidopropyl)dimethylammonio]-1-propanesulfonate (CHAPS) prevented MLC2 self-association; at a CHAPS concentration of 22.5 mM, the apparent

---

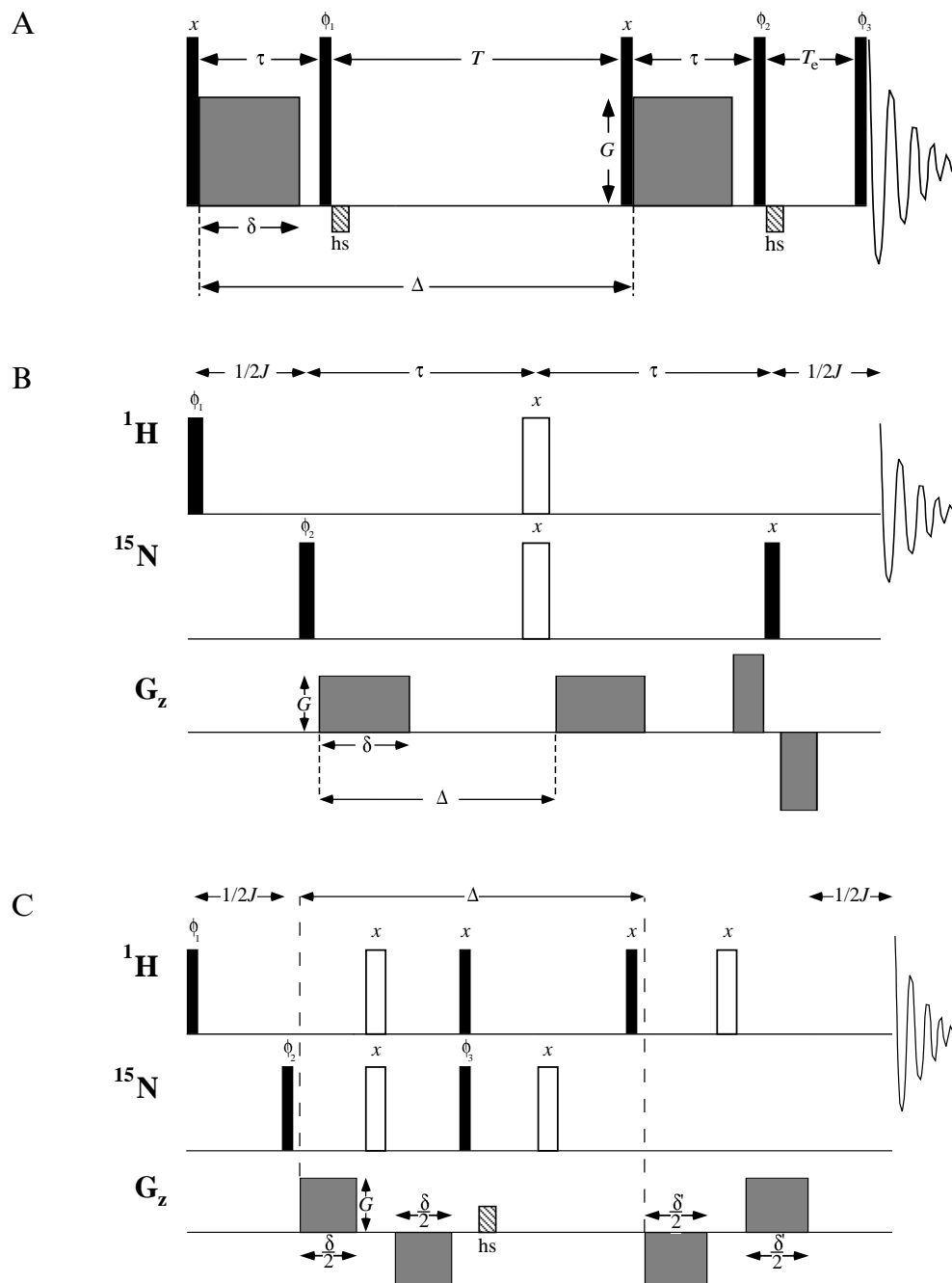*To whom correspondence should be addressed.

Fig. 1. Three pulse sequences for measuring $D_T$. Black and white bars represent $\pi/2$ and $\pi$ pulses, respectively, shaded boxes represent gradient pulses, and diagonally striped boxes represent homospoil pulses. (A) LED pulse sequence. Phase cycling was as follows: $\phi_1 = x,-x$; $\phi_2 = 2(x),2(-x)$; $\phi_3 = 4(x),4(y),4(-x),4(-y)$; receiver $= x,2(-x),x,y,2(-y),y,-x,2(x),-x,-y,2(y),-y$. (B) HMQC-type pulse sequence. The first two gradients define the diffusion period, while the final two select the desired coherence order. The two diffusion-gradient pulses were incremented by increasing either $\delta$ or G in each series of experiments. Phase cycling was as follows: $\phi_1 = x,-x$; $\phi_2 = 2(x), 2(-x)$; receiver $= x,2(-x),x$. (C) The ZZ pulse sequence. The two pairs of gradient pulses dephase and rephase magnetization, respectively, with the ratio of the lengths of the second pair set to select the desired heteronuclear MQ coherence. The gradient strengths (G) were incremented in each series of experiments. Phase cycling was as follows: $\phi_1 = 4(x),4(-x)$; $\phi_2 = x,-x$; $\phi_3 = 2(x),2(-x)$; receiver $= x,2(-x),x,-x,2(x),-x$.

molecular mass of MLC2 was ~23 kDa (Dingley et al., 1995), corresponding to a protein monomer plus seven molecules of bound CHAPS.

While the aforementioned studies employed $^1$H single-quantum (SQ) magnetization, it has been well documented that the $D_T$ of small molecules can be measured using homo- or heteronuclear multiple-quantum (MQ) coherences (Kay and Prestegard, 1986; Sotak, 1990; Kuchel and Chapman, 1993). The increasingly common use of uniform $^{15}$N and/or $^{13}$C labelling in macromolecular NMR raises the possibility of using heteronuclear MQ experiments to measure protein $D_T$ values, with a number of at-

tendant advantages over the corresponding ^{1}H SQ experiment. For example, most NMR studies require the protein to be in $H_2O$ in order to observe resonances from solvent exchangeable amide protons. This introduces a serious dynamic range problem associated with digitizing the solute signals in the presence of the large solvent resonance. A gradient-selected heteronuclear MQ filter incorporated into a diffusion experiment provides a convenient method for solvent suppression since it will select for magnetization arising from protons attached to the heteronucleus.

Another advantage of the use of MQ coherence in diffusion experiments is its increased sensitivity to the rate of molecular diffusion compared to SQ coherence. In the presence of an inhomogeneous field (i.e., a PFG), magnetization with a coherence order n dephases n times faster than magnetization with a coherence order of 1. The rate of signal attenuation observed in diffusion experiments depends on the extent to which the signal was dephased during the first PFG. Thus, diffusion experiments which monitor the decay of magnetization with a coherence order greater than 1 exhibit more rapid signal attenuation during the diffusion delay than would be observed in experiments monitoring SQ coherence (Zax and Pines, 1983; Kay and Prestegard, 1986). This property of MQ diffusion experiments makes them particularly suited to studying the diffusion of large macromolecules as either the PFG lengths or the diffusion period between the dephasing and rephasing PFGs can be shortened, thus minimizing magnetization losses due to relaxation.

As the size of the diffusant or the viscosity of the solution increases, the delay between the dephasing and rephasing gradients needs to be lengthened in order to accurately measure $D_T$. Hence, even when using MQ coherences, the necessarily long diffusion delay required for studying large molecules may lead to significant magnetization losses from relaxation. In the MQ diffusion experiments described to date, the magnetization of interest remains in the transverse plane for the duration of the diffusion period. Clearly, a pulse sequence that avoided the magnetization being transverse during the majority of the diffusion period, as in the ^{1}H PFG longitudinal eddy-current delay (LED) experiment (Gibbs and Johnson, 1991), would be advantageous for the study of large macromolecules (i.e., in cases where $T_1 \gg T_2$).

In this study, two pulse sequences employing MQ coherences for measuring the $D_T$ of macromolecules are presented and applied to three proteins: MLC2, the homodimeric Jun leucine zipper domain (JunLZ), and ubiquitin. One sequence has been described previously (Chapman and Kuchel, 1993) while the other has been developed to create longitudinal rather than transverse magnetization during the bulk of the diffusion period. We discuss the advantages of each pulse sequence relative to ^{1}H SQ experiments for measuring the $D_T$ of large macromolecules.

## Experimental

*Materials*

[$^{13}C$,$^{15}N$]-MLC2 was expressed and purified as previously described (Boey et al., 1994). [U-$^{13}C$,$^{15}N$]-human ubiquitin was purchased from VLI Research (Wayne, PA, U.S.A.). [U-$^{15}N$]-JunLZ was expressed and purified using a published method (Riley et al., 1994). Protein samples of depth no greater than 18 mm when placed in 5 mm susceptibility-matched microcells (Shigemi, Japan) were centered around the field-gradient coils.

*PFG NMR experiments*

All NMR spectra were acquired at 300 K on a Bruker DRX 500 MHz spectrometer. The magnetic field gradients were generated by an actively shielded coil assembled around the radiofrequency coils of a 5 mm triple resonance ($^{15}N$/$^{13}C$/$^{1}H$) probe. The probe was shown to provide linear field gradients up to ~500 mT m$^{-1}$ in the z direction over a length of 20 mm. The magnitude of the field gradients (G) was calibrated as previously described (Kuchel and Chapman, 1991).

Diffusion coefficients were measured using a modified version of the PFG LED sequence (Fig. 1A; Gibbs and Johnson, 1991), a modified version of the 1D heteronuclear multiple-quantum coherence (HMQC) diffusion experiment (Fig. 1B; Chapman and Kuchel, 1993), and a newly designed pulse sequence referred to as the ZZ sequence (Fig. 1C). $D_T$ measurements using the LED sequence were obtained from a series of 12 spectra in which the delay periods ($\tau = 10$–20 ms, T = 30–40 ms, $T_e = 6$ ms, and $\Delta = 50$ ms) and the gradient strength (G = 200–350 mT m$^{-1}$) were held constant but the length of the gradient ($\delta$) was incremented in steps ranging from 0.5 to 1.5 ms. $D_T$ measurements using the HMQC sequence were obtained from a series of 12–16 spectra in which the first pair of PFGs encompass the diffusion period ($\Delta$). These two PFGs were incremented in either $\delta$ or G in each series of experiments. Increments of ~25 mT m$^{-1}$ for G or 0.5–0.85 ms for $\delta$ were used. Each $\Delta$ and $\tau$ period ranged in length from 7 to 12 ms, unless otherwise stated. The desired coherence was selected by setting the ratio of the durations of the two final PFGs; zero-quantum (ZQ) and double-quantum (DQ) coherences were selected using the ratios $\gamma_H:(\gamma_H - \gamma_N)$ and $\gamma_H:(\gamma_H + \gamma_N)$, respectively, where $\gamma_H$ and $\gamma_N$ are the magnetogyric ratios of proton and nitrogen nuclei, respectively. The strength of the selection gradients was ~350 mT m$^{-1}$. $D_T$ measurements using the ZZ sequence were obtained from a series of 14 spectra in which the two pairs of PFGs encompass $\Delta$. Each pair of PFGs ranged in duration from 4 to 8 ms (depending on the protein size) and their strengths were incremented by ~25 mT m$^{-1}$ between sequential spectra in each series of experiments. ZQ or DQ coherence was selected by altering the ratio of the durations of two final PFGs as in the HMQC
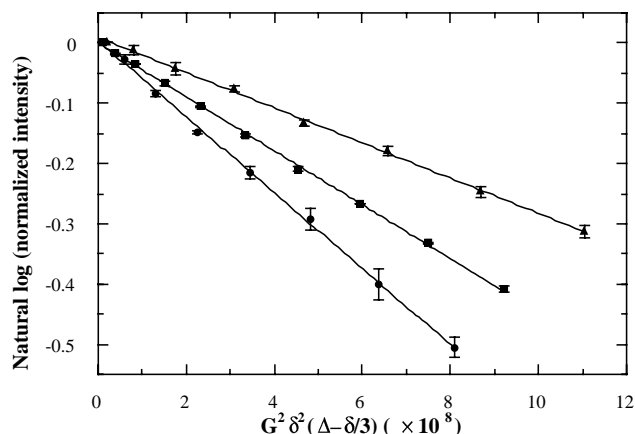
Fig. 2. Sensitivity of different coherence orders to field-gradient pulses. The natural log of the peak intensity of selected ubiquitin resonances is plotted as a function of $G^2\delta^2(\Delta-\delta/3)$ for a PFG LED experiment employing $^1H$ SQ coherence (■), and for HMQC experiments employing either $^1H$-$^{15}N$ ZQ (●) or $^1H$-$^{15}N$ DQ (▲) coherences. Each point represents the mean ± SD obtained from three peak measurements, and a weighted linear least-squares fit to each set of data is shown. The ratios of the slopes obtained from these fits are 0.65 and 1.36 for DQ/SQ and ZQ/SQ, respectively, which are in reasonable agreement with the theoretical values of 0.81 and 1.21 (see Eq. 1).

experiment. The homospoil (hs) field-gradient pulse was set to 70 mT m$^{-1}$ for 4 ms. In both the HMQC and ZZ experiments, the two $1/2J_{NH}$ periods were set to 5.44 ms.

Spectra consisted of 8192 data points for homonuclear experiments, but this was reduced to 2048 points in the heteronuclear experiments in order to keep the decoupler duty cycle at an acceptable level. FIDs were derived from 256–1024 transients and, prior to Fourier transformation, were multiplied by a decaying exponential function with a line-broadening factor of 1–5 Hz and zero-filled to 8192 real data points. For each series of experiments, a 'dummy' spectrum (G = 0 mT m$^{-1}$) was initially acquired to ensure that the sample had reached thermal equilibrium. Nitrogen decoupling using the GARP-1 sequence (Shaka et al., 1985) was applied during the acquisition period of the heteronuclear pulse sequences.

*Theory and analysis of PFG NMR experiments*

For unbounded diffusion of a molecule in an isotropic medium, the observed signal intensity (I) in a homonuclear diffusion experiment, relative to the signal obtained in the absence of PFGs ($I_0$), is given by (Stejskal and Tanner, 1965)

$$\frac{I}{I_0} = \exp(-n^2\gamma^2G^2D_T\delta^2(\Delta-\delta/3)) \qquad (1)$$

where G and δ are the magnitude and duration of the field-gradient pulses, respectively, Δ is the time between field-gradient pulses, γ is the magnetogyric ratio of the observed nucleus, and n is the coherence order selected. For a diffusion experiment monitoring the decay of het-

eronuclear MQ coherence, the $n^2\gamma^2$ term is replaced by $(n_H\gamma_H + n_X\gamma_X)^2$ (Kuchel and Chapman, 1993), where $\gamma_X$ is the magnetogyric ratio of the heteronucleus and $n_i$ is the coherence order of nucleus i. This term simplifies to $(\gamma_H + \gamma_N)^2$ for $^1H$-$^{15}N$ DQ coherence and $(\gamma_H - \gamma_N)^2$ for $^1H$-$^{15}N$ ZQ coherence.

Non-linear regression of Eq. 1 onto the data, using x $= n^2\gamma^2G^2\delta^2(\Delta-\delta/3)$ as the independent variable, yields $D_T$ and an estimate of its standard deviation (σ). A weighted (where appropriate) three-parameter fit of the form $I = I_\infty + I_0\exp(-D_Tx)$ was used to fit the data, where $I_0$ and $I_\infty$ are the normalized resonance intensities at zero and infinite time, respectively. $D_T$ values were calculated independently from six resonances in each case, and the weighted average and group standard deviation ($D_m \pm \sigma_m$) were calculated, using $1/\sigma^2$ as the weights (Spiegel, 1972). When more than one experiment was performed using a particular pulse sequence, the weighted mean and group standard deviation from each experiment was calculated to give the final $D_T$.

*Calculation of the effective molecular masses of MLC2, ubiquitin, and JunLZ*

The translational diffusion coefficient is related to the apparent molecular mass, $M_{app}$, of the diffusing species by the following equation (Dingley et al., 1995):

$$M_{app} = \left(\frac{kT}{6\pi\eta FD_T}\right)^3 \left(\frac{4\pi N_A}{3[\bar{v}_2 + \delta_1\bar{v}_1]}\right) \qquad (2)$$

where k is the Boltzmann constant (J K$^{-1}$), T is the temperature (K), η is the viscosity of the solution taken to be water at 300 K ($8.513 \times 10^{-4}$ kg m$^{-1}$ s$^{-1}$; Weast, 1984), $D_T$ is the translational diffusion coefficient (m$^2$ s$^{-1}$), $N_A$ is Avogadro's number (mol$^{-1}$), $\bar{v}_2$ is the partial specific volume of the molecule (m$^3$ kg$^{-1}$), $\delta_1$ is the fractional amount of water bound to the molecule (g $H_2O$ per g diffusant), and $\bar{v}_1$ is the partial specific volume of solvent water (m$^3$ kg$^{-1}$). The dimensionless Perrin factor, F, which relates to the shape of the molecule, is equal to the ratio of the frictional coefficient of the diffusant (f) to that of a hard sphere of equivalent mass ($f_{sphere}$).

The molecular masses of MLC2 + 25 mM CHAPS, JunLZ, and ubiquitin were calculated using partial specific volumes of $0.73 \times 10^{-3}$, $0.74 \times 10^{-3}$, and $0.68 \times 10^{-3}$ m$^3$ kg$^{-1}$, respectively, which were calculated on the basis of amino acid composition (Perkins, 1986). The F value for MLC2 was calculated to be 1.030 (Dingley et al., 1995). An F value of 1.003 was calculated for ubiquitin using the coordinates of the crystal structure (Vijay-Kumar et al., 1987; Brookhaven accession code 1ubq), while a value of 1.096 was calculated for JunLZ from the NMR solution structure (Junius et al., 1996; Brookhaven accession code 1jun). Most proteins have hydration ($\delta_1$) values of 0.30–0.40 g $H_2O$ per g protein (Cantor and Schimmel, 1980); in this study we used a value of 0.34, correspon-

A

$\Delta = 9.5$ ms

C

$\Delta = 52$ ms

B

D



10  9  8  7  6  5
$^1$H chemical shift (ppm)

10  9  8  7  6  5
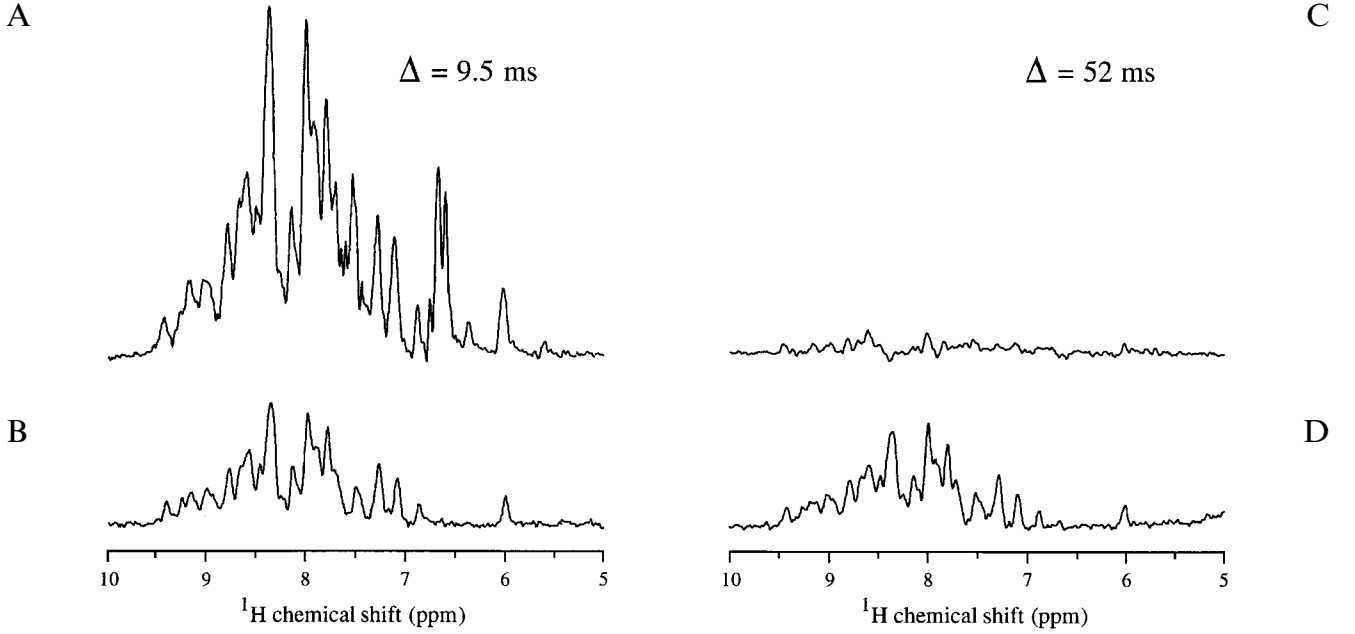$^1$H chemical shift (ppm)

Fig. 3. Amide-proton region of the $^1$H NMR spectrum of ubiquitin collected using short or long diffusion periods with either the HMQC (A and C) or ZZ (B and D) pulse sequences. $^1$H-$^{15}$N ZQ coherence was selected in all experiments. (A) HMQC sequence with $\Delta = 9.5$ ms; (B) ZZ sequence with $\Delta = 9.5$ ms; (C) HMQC sequence with $\Delta = 52$ ms; (D) ZZ sequence with $\Delta = 52$ ms. The HMQC experiment, as predicted, has better signal-to-noise at short values of $\Delta$ (compare spectra A and B). However, at the longer diffusion period, the signal intensity in the HMQC spectrum (C) is degraded by fast transverse relaxation and homonuclear coupling evolution. In contrast, the spectrum collected using the ZZ pulse sequence at $\Delta = 52$ ms (D) has no phase distortions, and the signal-to-noise ratio is much higher due to longitudinal storage of the magnetization for the majority of the diffusion period.

ding to a protein hydration shell approximately one water molecule thick.

## Results

*Sensitivity of heteronuclear PFG experiments*

While $^1$H SQ coherences can be used to measure the $D_T$ of small proteins (e.g., the PFG LED experiment), MQ coherences are likely to be more useful for studying larger proteins because of their faster dephasing during a field-gradient pulse. Figure 2 shows the attenuation of $^1$H SQ, $^1$H-$^{15}$N DQ, and $^1$H-$^{15}$N ZQ coherences for ubiquitin as a function of field-gradient strength. Clearly, $^1$H-$^{15}$N ZQ coherence is more sensitive to field gradients than the other two coherences. Thus, an experiment selecting ZQ coherence would be useful for measuring $D_T$ in larger, more slowly diffusing proteins, where it becomes more difficult to attenuate the NMR signal without losing signal-to-noise due to relaxation processes.

As mentioned previously, it would also be desirable to store the magnetization longitudinally during the diffusion delay period to minimize losses due to transverse relaxation. This prompted us to develop the ZZ sequence shown in Fig. 1C. The following product operator description of the ZZ experiment ignores evolution of chemical shifts as they are refocussed over the course of the pulse sequence. SQ magnetization created by the first $^1$H $\pi/2$ pulse evolves to become antiphase with respect to the one-bond heteronuclear coupling at the end of the 1/2J

period. The $^{15}$N $\pi/2$ pulse then creates a mixture of heteronuclear DQ and ZQ coherences:

$$2I_xS_z \xrightarrow{(\pi/2)S_x} -2I_xS_y \equiv$$

$$-\frac{1}{2i}(I^+S^+ - I^+S^- + I^-S^+ - I^-S^-)$$

The first $\gamma G_z t$-$\pi_H$,$\pi_N$-$\gamma \overline{G}_z t$ element can be treated as a single gradient in which the simultaneous $\pi$ pulses that split the field-gradient pulses ensure that $^1$H and $^{15}$N chemical shift evolution is refocussed. These field-gradient pulses dephase all transverse magnetization according to the length and strength of the gradient and the order of the coherences present. Unlike the HMQC experiment, the ZZ sequence combines the field-gradient pulses that measure the diffusion coefficient with those that select the desired coherence order, thereby shortening the time that the magnetization spends in the transverse plane. Thus, we have

$$-\frac{1}{2i}(I^+S^+ - I^+S^- + I^-S^+ - I^-S^-) \xrightarrow{\gamma G_z t - \pi I_x \pi S_x - \gamma \overline{G}_z t}$$

$$-\frac{1}{2i}(I_x - iI_y)(S_x - iS_y)\exp(\phi_1)$$

$$+\frac{1}{2i}(I_x - iI_y)(S_x + iS_y)\exp(\phi_2)$$

$$-\frac{1}{2i}(I_x + iI_y)(S_x - iS_y)\exp(\phi_3)$$

$$+\frac{1}{2i}(I_x + iI_y)(S_x + iS_y)\exp(\phi_4)$$

where $\phi_1 = -\phi_I - \phi_S$, $\phi_2 = -\phi_I + \phi_S$, $\phi_3 = \phi_I - \phi_S$, $\phi_4 = \phi_I + \phi_S$, $\phi_I = i\gamma_I G_z t$, and $\phi_S = i\gamma_S G_z t$.

The simultaneous $\pi/2$ pulses place the $I_y S_y$ terms along the z-axis to give longitudinal two-spin order ($I_z S_z$), while the remaining product operator terms (i.e., $I_z S_x$, $I_x S_z$, and $I_x S_x$) are left in the transverse plane and are destroyed by the homospoil field-gradient pulse:

$$-\frac{1}{2i}(I_x - iI_y)(S_x - iS_y)\exp(\phi_1)$$
$$+\frac{1}{2i}(I_x - iI_y)(S_x + iS_y)\exp(\phi_2)$$
$$-\frac{1}{2i}(I_x + iI_y)(S_x - iS_y)\exp(\phi_3)$$
$$+\frac{1}{2i}(I_x + iI_y)(S_x + iS_y)\exp(\phi_4) \xrightarrow{(\pi/2)I_x (\pi/2)S_x - \text{homospoil}}$$
$$\frac{1}{2i}I_z S_z \exp(\phi_1) + \frac{1}{2i}I_z S_z \exp(\phi_2)$$
$$-\frac{1}{2i}I_z S_z \exp(\phi_3) - \frac{1}{2i}I_z S_z \exp(\phi_4)$$

+ other terms destroyed by the homospoil

Thus, only the $I_z S_z$ term, which does not suffer from rapid relaxation and does not evolve under heteronuclear or homonuclear J-couplings, is present during the remainder of the molecular diffusion period. At the end of the diffusion period, the magnetization is made transverse by a $^1$H $\pi/2$ pulse (i.e., $-I_y S_z$). The second $\gamma \overline{G}_z t' \text{-} \pi_H \text{-} \gamma G_z t'$ pulse train rephases only one of the four gradient-labelled components; assuming the gradients are set to rephase ZQ coherence, we obtain

$$\frac{1}{2i}I_y S_z \exp(\phi_2) \equiv -\frac{1}{4}(I^+ - I^-)S_z \exp(\phi_2)$$
$$\xrightarrow{\gamma \overline{G}_z t' \text{-} \pi_H \text{-} \gamma G_z t'} -\frac{1}{4}I^- S_z$$

The antiphase proton magnetization is allowed to refocus during the second $1/2J_{NH}$ period:

$$-\frac{1}{4}I^- S_z \equiv -\frac{1}{4}(I_x - iI_y)S_z \xrightarrow{\pi I_z S_z} -\frac{i}{8}I^-$$

If relaxation and pulse imperfections are neglected, the sensitivity of this experiment is theoretically half that of the HMQC and PFG LED pulse sequences. The $^{15}$N $\pi$ pulse at the midpoint of the longitudinal storage period refocusses any heteronuclear cross relaxation and $^1$H-$^1$H cross relaxation between amide and non-amide protons, thus avoiding a potential loss in sensitivity resulting from these relaxation pathways. Note, however, that the presence of dipolar cross relaxation will not affect the value of $D_T$ derived from the experiment.

A comparison of Figs. 3A and 3B shows that for short diffusion delay periods ($\Delta = 9.5$ ms) the amide region of the $^1$H NMR spectrum of ubiquitin collected using the

HMQC pulse sequence has approximately twofold greater sensitivity than the equivalent spectrum collected using the ZZ pulse sequence. This corresponds to the theoretical prediction if relaxation losses and J-coupling evolution in the HMQC experiment are ignored. However, one would expect that, when using longer diffusion periods ($\geq 30$ ms) to study larger species, the sensitivity of the HMQC experiment would be compromised by transverse relaxation losses and J-coupling evolution during the diffusion period. In contrast, transverse relaxation losses are minimized in the ZZ pulse sequence through longitudinal storage of the magnetization during most of $\Delta$. This is borne out by a comparison of the spectra of ubiquitin obtained using the HMQC sequence (Fig. 3C) and the ZZ sequence (Fig. 3D), with $\Delta$ set to 52 ms in both cases. Whereas the signal intensity in the HMQC experiment is substantially reduced when $\Delta$ is increased from 9.5 to 52 ms (compare Figs. 3A and C), the signal intensity in the ZZ experiment is only marginally worse (compare Figs. 3B and D).
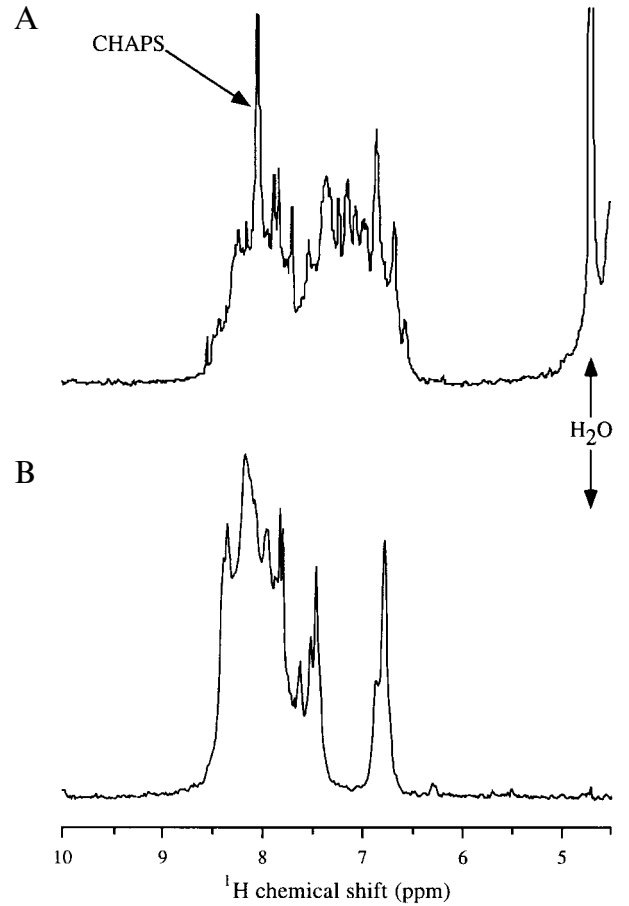


Fig. 4. Amide-proton region of the $^1$H NMR spectrum of MLC2 in the presence of 25 mM CHAPS. Spectra were acquired using either the (A) LED (512 scans) or (B) HMQC (1024 scans) pulse sequences, demonstrating both the superior solvent suppression and the filtering of the unlabelled CHAPS signal in the latter experiment. Note that the signals arising from the aromatic residues present in MLC2 (ca. 6.7–7.5 ppm) are also filtered out in the HMQC experiment.

TABLE 1

MEASURED $D_T$ AND CALCULATED $M_{app}$ OF JunLZ, MLC2 IN THE PRESENCE OF 25 mM CHAPS, AND UBIQUITIN

|  | Experiment | $D_T$ ($\times 10^{10}$ m$^2$ s$^{-1}$) | $M_{app}$ (kDa) | Theoretical M (kDa) |
|---|---|---|---|---|
| Ubiquitin | LED | $1.690 \pm 0.009^a$ | 8.6 | |
| | HMQC | $1.768 \pm 0.016$ | 7.6 | 8.6 |
| | ZZ | $1.752 \pm 0.025$ | 7.8 | |
| JunLZ | LED | $1.360 \pm 0.010$ | 12.2 | |
| | HMQC | $1.355 \pm 0.006$ | 12.3 | 10.2 |
| | ZZ | $1.384 \pm 0.009$ | 11.6 | |
| MLC2 | LED | $1.086 \pm 0.090^b$ | 24.8 | |
| | HMQC | $1.107 \pm 0.070^b$ | 23.4 | $23.5^c$ |
| | ZZ | $1.130 \pm 0.005$ | 25.7 | |

[a] Errors reflect *only* the contribution from spectral noise and do not account for potential systematic errors in parameters such as gradient strength and duration.
[b] Diffusion measurement recorded at 298 K.
[c] M calculated assuming one CHAPS micelle is bound to MLC2.

*Removal of unwanted signals*

The ability to remove undesirable solvent and solute resonances in diffusion experiments employing gradient selection of MQ coherences, without the requirement of presaturation, constitutes another advantage of these sequences over $^1$H SQ diffusion experiments. For example, Fig. 4A shows the amide region of a PFG LED experiment carried out on MLC2 in the presence of 25 mM CHAPS. A dominant signal in this region from the detergent interferes with the measurement of MLC2 resonance intensities. However, this signal is effectively eliminated by the gradient-selected heteronuclear filter in the HMQC pulse sequence (Fig. 4B). In addition, the solvent suppression in the HMQC experiment is superior to that in the LED experiment, again due to the selection of heteronuclear ZQ coherence in the former experiment (compare the H$_2$O signal in Figs. 4A and B). Note that solvent suppression in the ZZ experiment is approximately an order of magnitude poorer than the HMQC (data not shown), probably as a result of using split gradient pulses (i.e., gradient-$\pi_H$,$\pi_N$-gradient; see Fig. 1C); any component of the water magnetization that does not experience a perfect $\pi$ pulse is not completely dephased and is consequently observed during acquisition.

*Measurement of $D_T$*

LED, HMQC, and ZZ diffusion experiments were used to measure the $D_T$ of MLC2 (in the presence of 25 mM CHAPS), ubiquitin, and JunLZ. Resonance intensities arising from the backbone amide protons of the proteins were measured as a function of the duration or strength of the field-gradient pulses. For all diffusion measurements made using the HMQC and ZZ pulse sequences, $^1$H-$^{15}$N ZQ coherence was selected because of its greater sensitivity to the field-gradient pulses (see Fig. 2). Each diffusion experiment consisted of 11–16 spectra acquired with different gradient strength or duration; the intensities of six peaks were measured in each spectrum and the $D_T$ was calculated for each peak by non-linear regression of Eq. 1 onto the data.

The $D_T$ values measured for each of the three proteins using the two heteronuclear PFG pulse sequences and the $^1$H LED pulse sequence are very similar (see Table 1). These values were used to estimate $M_{app}$ using Eq. 2. The $M_{app}$ calculated for ubiquitin using the $D_T$ values measured from each pulse sequence were similar to the theoretical value for a monomer. The calculated $M_{app}$ for the JunLZ homodimer is slightly higher than the theoretical molecular mass of 10.2 kDa. The three $D_T$ values for MLC2 used to calculate the apparent molecular mass are similar, and compare well with the theoretical value of 23.5 kDa assuming one CHAPS micelle is bound to one MLC2 molecule (Dingley et al., 1995).

**Discussion and Conclusions**

This paper describes two heteronuclear PFG NMR experiments that can be used to measure the translational diffusion coefficients of macromolecules and thereby estimate their effective molecular mass in solution. The determination of the aggregation state of, for example, a protein constitutes a necessary prerequisite to structural studies, and these experiments represent a convenient way to obtain this information using the actual NMR sample, in cases where $^{15}$N labelling is employed.

These heteronuclear experiments have several advantages over their $^1$H counterparts. For certain coherences (e.g., $^1$H-$^{15}$N ZQ coherence), there is an increase in the rate of dephasing under the influence of the field gradient, compared to $^1$H SQ coherence. This increase allows either the diffusion period, $\Delta$, or the gradient lengths to be shortened, or, alternatively, permits the translational diffusion of larger species to be measured. Selection of heteronuclear MQ coherence also allows undesirable resonances arising from unlabelled species to be filtered out. The most obvious example of this is the solvent H$_2$O signal. The spectra in Fig. 4 show that the solvent signal is more effectively suppressed in the heteronuclear experiment than in the LED experiment. Further, in the case of MLC2 in the presence of CHAPS, the relatively large detergent signal in the amide-proton region of the spectrum was removed, permitting an accurate measurement of MLC2 signal intensities.

Of these two heteronuclear pulse sequences, the HMQC experiment is better suited to the measurement of $D_T$ for smaller macromolecules because it achieves better signal-to-noise. However, for larger species, where longer diffusion periods ($\geq$30 ms) are required to achieve sufficient signal attenuation, the ZZ experiment is preferable. This is because the magnetization is present as zz-order for most of the diffusion period, thereby substantially allevi-

ating the problems of fast transverse relaxation and homonuclear $^1$H-$^1$H J-coupling evolution present in the HMQC experiment. The potentially detrimental effects of heteronuclear dipolar cross relaxation and cross relaxation between amide and non-amide protons are circumvented in the ZZ experiment by the application of a $\pi$ pulse on $^{15}$N at the midpoint of the longitudinal storage period. The combined effects of these measures can be seen in the very similar resonance intensities observed for ZZ experiments recorded with diffusion periods of 9.5 and 52 ms (compare Figs. 3B and D).

We utilized $^1$H-$^{15}$N ZQ coherence in the heteronuclear diffusion experiments as it is ~20% more sensitive to the field-gradient pulses than $^1$H SQ coherence. In comparison, $^1$H-$^{13}$C DQ coherence is ~60% more sensitive to field-gradient pulses than $^1$H SQ coherence. However, we observed severe phase distortions in the spectra due to the evolution of the homonuclear $^{13}$C and $^1$H J-couplings when we employed $^1$H-$^{13}$C DQ coherence in either of the heteronuclear experiments (data not shown). Refocussing of the relatively large $^1J_{CC}$ coupling evolution can be achieved by setting the $2\tau$ period in the HMQC pulse sequence to $1/J_{CC}$ (~28 ms), although this leads to substantial signal loss from transverse relaxation. Furthermore, the evolution of $^nJ_{HH}$ couplings during this period still leads to extensive phase distortions. The problem of $^1$H-$^1$H coupling evolution is significantly greater in the $^{13}$C compared to $^{15}$N versions of these experiments since, in general, carbon-bound protons exhibit a larger number of homonuclear J-couplings. The ZZ experiment partially alleviates this problem by limiting the length of time for which the magnetization is transverse, but phase distortions still arise from limited coupling evolution during the finite field-gradient periods (4–8 ms).

The values of $D_T$ obtained from the two heteronuclear PFG NMR pulse sequences agree well with the values obtained from the homonuclear LED experiment, demonstrating that they are suitable alternatives to the LED experiment (Altieri et al., 1995; Dingley et al., 1995) for measuring the $D_T$ of macromolecules. It is of interest that the diffusion coefficients obtained for JunLZ predict molecular masses which are ca. 15–20% higher than the calculated value. This could be due to a small amount of aggregation, or perhaps it is a reflection of the difficulty in predicting very accurate molecular masses from diffusion data when dealing with asymmetric molecules that cannot necessarily be modelled as smooth ellipsoids. This could arise simply from an unusual molecular shape, a high degree of surface rugosity, or an unusual degree of surface hydration. Consequently, the methods presented in this and our previous paper (Dingley et al., 1995) are not suitable for accurate mass determinations, but are rather tools with which to distinguish substantial changes

in molecular mass that may occur as a consequence of either specific or non-specific aggregation. These techniques could therefore potentially be used to monitor and quantitate specific bimolecular binding events, such as the formation of a protein–drug or DNA–drug complex.

## Acknowledgements

## References

Altieri, A.S., Hinton, D.P. and Byrd, R.A. (1995) *J. Am. Chem. Soc.*, **117**, 7566–7567.

Boey, W., Huang, W., Bennetts, B., Sparrow, J., dos Remedios, C. and Hambly, B. (1994) *Eur. J. Biochem.*, **219**, 603–610.

Cantor, C.R. and Schimmel, P.R. (1980) *Biophysical Chemistry. Part II: Techniques for the Study of Biological Structure and Function*, Freeman, New York, NY, U.S.A., pp. 539–590.

Chapman, B.E. and Kuchel, P.W. (1993) *J. Magn. Reson.*, **A102**, 105–109.

Dingley, A.J., Mackay, J.P., Morris, M.B., Chapman, B.E., Kuchel, P.W., Hambly, B.D. and King, G.F. (1995) *J. Biomol. NMR*, **6**, 321–328.

Gibbs, S.J. and Johnson Jr., C.S. (1991) *J. Magn. Reson.*, **93**, 395–402.

Junius, F.K., O'Donoghue, S.I., Nilges, M., Weiss, A.S. and King, G.F. (1996) *J. Biol. Chem.*, **271**, 13663–13667.

Kay, L.E. and Prestegard, J.H. (1986) *J. Magn. Reson.*, **67**, 103–113.

King, G.F. and Mackay, J.P. (1996) In *NMR in Drug Design* (Ed., Craik, D.J.), CRC Press, Boca Raton, FL, U.S.A., pp. 101–200.

Kuchel, P.W. and Chapman, B.E. (1991) *J. Magn. Reson.*, **94**, 574–580.

Kuchel, P.W. and Chapman, B.E. (1993) *J. Magn. Reson.*, **A101**, 53–59.

Perkins, S.J. (1986) *Eur. J. Biochem.*, **157**, 169–180.

Riley, L.G., Junius, F.K., Swanton, M.K., Vesper, N.A., Williams, N.K., King, G.F. and Weiss, A.S. (1994) *Eur. J. Biochem.*, **219**, 877–886.

Shaka, A.J., Barker, P.B. and Freeman, R. (1985) *J. Magn. Reson.*, **64**, 547–552.

Sotak, C.H. (1990) *J. Magn. Reson.*, **90**, 198–204.

Spiegel, M.R. (1972) *Theory and Problems of Statistics*, McGraw-Hill, New York, NY, U.S.A.

Stejskal, E.O. and Tanner, J.E. (1965) *J. Chem. Phys.*, **42**, 288–292.

Vijay-Kumar, S., Bugg, C.E. and Cook, W.J. (1987) *J. Mol. Biol.*, **194**, 531–544.

Weast, R.C. (Ed.) (1984) *CRC Handbook of Chemistry and Physics*, 65th ed., CRC Press, Boca Raton, FL, U.S.A., p. F-37.

Zax, D. and Pines, A. (1983) *J. Chem. Phys.*, **78**, 6333–6334.